DOI: 10.1002/cmdc.201100121

Novel 2-Substituted Quinolin-4-yl-benzenesulfonate Derivatives: Synthesis, Antiproliferative Activity, and Inhibition of Cellular Tubulin Polymerization

Rajesh Kakadiya,[a] Yi-Chen Wu,[b] Huajin Dong,[c] Hsiao-Hui Kuo,[b] Ling-Huei Yih,*[b] Ting-Chao Chou,[c] and Tsann-Long Su*[a, d]

A series of 2-substituted quinolin-4-yl-benzenesulfonate derivatives were synthesized for the purpose of evaluating antiproliferative activity. Structure–activity relationships of the newly synthesized compounds against human lymphoblastic leukemia and various solid tumor cell growths in culture are discussed. Of these derivatives, 2-phenyl-6-pyrrolidinyl-4-quinoline sulfonate analogues **10f**, **10g**, and **10k**, and 4′-nitrophenyl sulfonate **10m** exhibit superior cytotoxicity over other sulfonates. The antiproliferative activities of these compounds correlate well with their abilities to induce mitotic arrest and apoptosis. Mechanistic studies indicate that they target the vinblastine binding site of tubulin and inhibit cellular tubulin polymerization. Hence, these compounds induce the formation of aberrant mitotic spindles and mitotic arrest, resulting in intensive apoptosis. The tested compounds were shown to be poor substrates for membrane multidrug resistance transporters. The present studies suggest that these newly synthesized compounds are promising tubulin polymerization inhibitors and are worthy of further investigation as antitumor agents.

Introduction

Microtubules are long, rigid, cylindrical tubes with walls that are formed by the assembly of α- and β-tubulin subunits. Most microtubules undergo continuous polymerization and depolymerization through the addition of tubulin subunits at one end and dissociation at the other end. Microtubules are essential for maintaining cell shape and polarity, the intracellular transport of vesicles and organelles, and the beating of cilia and flagella.[1,2] During eukaryotic cell division, microtubules form mitotic spindles, which align replicated chromosomes to the equatorial plane and mediate the subsequent segregation of chromosomes to the two daughter cells.[3] As microtubules play an important role in cell division, they are potential targets for the development of chemotherapeutic drugs which target rapidly dividing cancer cells.[4,5] These drugs interfere with the polymerization–depolymerization properties of microtubules to prevent cell cycle progression, inducing the cells to undergo programmed cell death.[2,6,7]

Numerous small molecules with diverse structures and potent antitumor activity were identified as effective microtubule-targeted drugs in recent years. Most of these agents are naturally occurring products, such as vinca alkaloids (vincristine, vinblastine, and vinorelbine),[8] taxanes (paclitaxel and docetaxel),[9] and epothilones,[10] which have all been proven to successfully treat a wide variety of human cancers. These agents act by either inhibiting the polymerization of tubulin (vinca alkaloids and colchicines) or preventing the disassembly of microtubules (taxanes and epothilones). Accordingly, three important binding domains on β-tubulin, namely the vinca binding site, the taxane binding site, and the colchicine binding site, have been identified.[11] Compounds which bind to the vinca or colchicine binding sites inhibit cancer cell proliferation and tubulin assembly by destabilizing microtubules.[2,12] In contrast, compounds which bind to the taxane binding site prevent microtubule disassembly by stabilizing microtubules.[12] However, owing to high toxicity, poor bioavailability, and synthetic difficulty, taxanes and vinblastine have limited clinical applications. Moreover, they induce overexpression of transmembrane efflux proteins that pump out antimitotic inhibitors, resulting in decreased potency and rapid development of multidrug resistance (MDR).[13] Consequently, searching for compounds which target tubulin without producing cross-resistance to taxane or vinblastine is an urgent need in the development of new anticancer agents.

Combretastatin A-4 (CA-4, **1**, Figure 1), isolated from *Combretum caffrum*,[14] exhibits potent cytotoxicity with a broad spec-

[a] *Dr. R. Kakadiya, Prof. T.-L. Su*
Institute of Biomedical Sciences
Academia Sinica, Taipei 11529 (Taiwan)
Fax: (+886) 2-27829142
E-mail: tlsu@ibms.sinica.edu.tw

[b] *Y.-C. Wu, H.-H. Kuo, Dr. L.-H. Yih*
Institute of Cellular and Organismic Biology
Academia Sinica, Taipei 11529 (Taiwan)
Fax: (+886) 2-27858059
E-mail: lhyih@gate.sinica.edu.tw

[c] *Dr. H. Dong, Dr. T.-C. Chou*
Preclinical Pharmacology Core Laboratory
Molecular Pharmacology and Chemistry Program
Memorial Sloan-Kettering Cancer Center, New York, NY 10021 (USA)

[d] *Prof. T.-L. Su*
Graduate Institute of Pharmaceutical Chemistry
China Medical University, Taichung (Taiwan)

Supporting information for this article is available on the WWW under http://dx.doi.org/10.1002/cmdc.201100121.

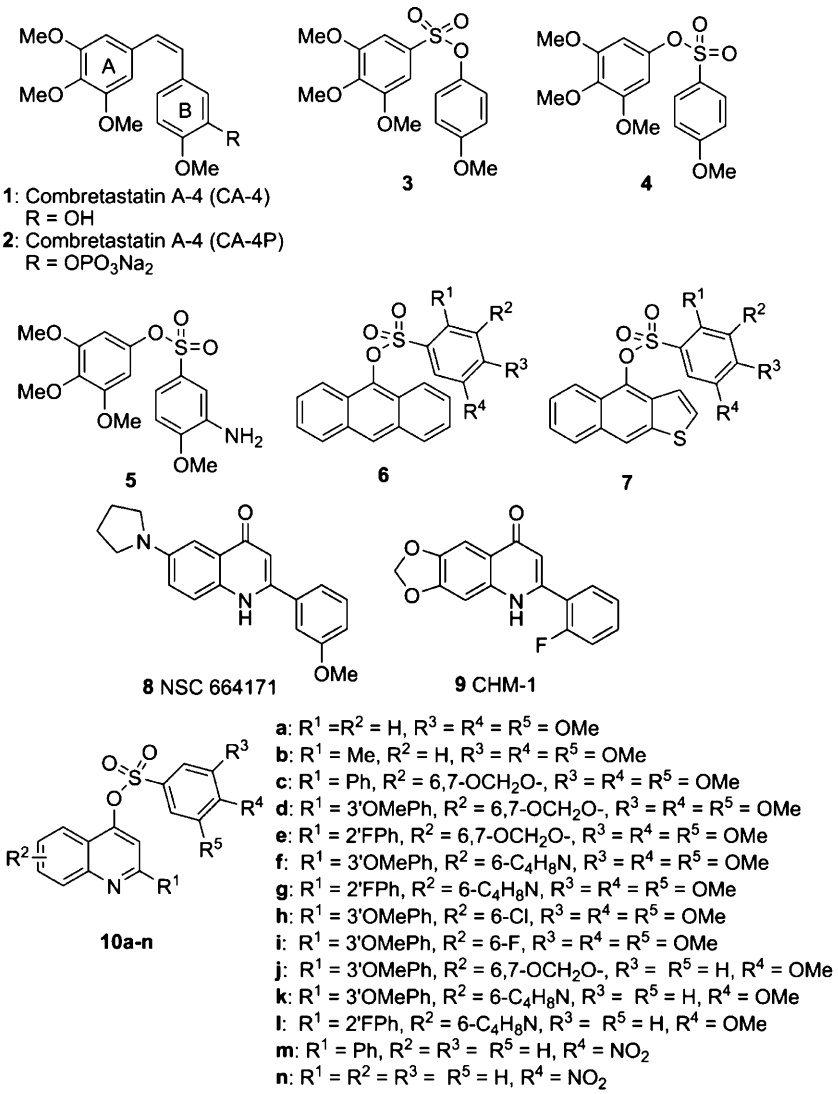

Figure 1. Structure of combretastatin A-4 (CA-4, **1**), water-soluble prodrug CA-4P (**2**), sulfonate analogues **3**–**7**, 2-phenylquinolones **8** and **9**, and the recently generated 2-substituted quinoline sulfonates **10a**–**n**.

trum of antitumor activity.[15–17] CA-4 and related derivatives are microtubule inhibitors which target the colchicine binding site and exhibit low toxicity profiles.[18,19] Despite its potent cytotoxic and antitubulin activities, CA-4 failed to exhibit potent antitumor efficacy in animal models due to its limited water solubility (poor bioavailability).[20] Accordingly, the water-soluble prodrug, CA-4 disodium phosphate (**2**, CA-4-DP, Figure 1), was synthesized and found to have potent antiangiogenic and tubulin inhibition effects.[21,22] This compound is currently undergoing phase I/II clinical trials.[23,24] Because of its interesting antitumor activity, a number of CA-4 analogues have been synthesized with modifications to ring A, ring B, and the bridge.[25] It was also demonstrated that the *cis* isomer is more cytotoxic than the corresponding *trans* isomer. Although none of the compounds with a modified bridge exhibit more potent bioactivity than CA-4, some analogues still retain high tubulin polymerization activity and cytotoxicity.

Among antimitotic CA-4 analogues, Gwaltney et al.[26] synthesized a series of CA-4-like sulfonates by introducing a sulfonate functional group as a tether between the two aryl rings (**3**–**5**, Figure 1), which are structural features of CA-4. Many of the sulfonates were reported to have excellent antitumor activities as well as inhibitory effects against tubulin polymerization. Structure–activity relationship (SAR) studies of CA-4-like sulfonates demonstrated that replacement of the *cis* olefin and the aryl moieties with a sulfonate functionality and heterocyclic ring, respectively, are well tolerated. The orientation of the sulfonate group relative to the two aryl rings makes little difference in antitumor activity. For example, compound **3** (Figure 1) has a sulfonate moiety adjacent to the 3,4,5-trimethoxyphenyl ring and exhibits greater inhibitory activity than corresponding compound **4** toward human colon adenocarcinoma HCT-15 cell growth in vitro, with IC_{50} values of 36 and 250 nM, respectively. However, compound **5**, which has a 3′-amino-4′-methoxy-substituted pattern was shown to be the most potent cell growth inhibitor, with IC_{50} values of 4.1 and 2.7 nM against HCT-15 and H460 cells, respectively. CA-4 exhibited IC_{50} values of 1.7 and 3 nM, respectively, against the same cell lines. Recently, Zuse et al.[27] synthesized sulfonate derivatives of anthracenone (**6**, Figure 1) and naphthothiophenone (**7**), which can be considered anthracenoid analogues of CA-4. These derivatives displayed potent cytotoxicity and microtubule-disrupting activity, and are most likely to interact with tubulin at the colchicine binding site.

The 2-phenyl-4-quinolones are another group of molecules which display anticancer activity through the inhibition of tubulin polymerization. Kuo, Lee, and colleagues synthesized a series of 2-phenyl-4-quinolone derivatives,[28–32] including NSC 664171 (**8**, Figure 1) and CHM-1 (**9**, Figure 1), which were shown to have potent antitumor activity. These agents inhibited the growth of NCI tumor cell lines within a small range of nanomolar concentrations. Both compounds are potent inhibitors of tubulin polymerization and have cytotoxicities similar to that of CA-4.

As previously mentioned, the sulfonate group can replace the *cis* olefin bridge of CA-4 while preserving cytotoxicity. However, the two moieties attached to the sulfonate functionality can be varied, so we designed and synthesized a series of 2-substituted-quinolin-4-yl-benzenesulfonates for antitumor evaluation which, in theory, could be enzymatically hydrolyzed to release the biologically active quinolones. The results show that the newly synthesized quinoline sulfonates exhibit significant cytotoxicity against human lymphoblastic leukemia and inhibit growth of various solid tumor cells in culture. Additionally, we found that these agents target the vinblastine site of tubulin and inhibit cellular tubulin polymerization. Herein, we report the antitumor activity and mechanism of action of these new sulfonates.

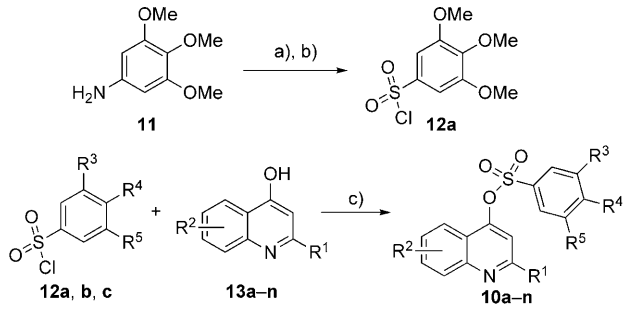

12a: $R^3 = R^4 = R^5 = OMe$
12b: $R^3 = R^5 = H$, $R^4 = OMe$
12c: $R^3 = R^4 = H$, $R^5 = NO_2$

a: $R^1 = R^2 = H$, $R^3 = R^4 = R^5 = OMe$
b: $R^1 = Me$, $R^2 = H$, $R^3 = R^4 = R^5 = OMe$
c: $R^1 = Ph$, $R^2 = 6,7\text{-}OCH_2O\text{-}$, $R^3 = R^4 = R^5 = OMe$
d: $R^1 = 3'OMePh$, $R^2 = 6,7\text{-}OCH_2O\text{-}$, $R^3 = R^4 = R^5 = OMe$
e: $R^1 = 2'FPh$, $R^2 = 6,7\text{-}OCH_2O\text{-}$, $R^3 = R^4 = R^5 = OMe$
f: $R^1 = 3'OMePh$, $R^2 = 6\text{-}C_4H_8N$, $R^3 = R^4 = R^5 = OMe$
g: $R^1 = 2'FPh$, $R^2 = 6\text{-}C_4H_8N$, $R^3 = R^4 = R^5 = OMe$
h: $R^1 = 3'OMePh$, $R^2 = 6\text{-}Cl$, $R^3 = R^4 = R^5 = OMe$
i: $R^1 = 3'OMePh$, $R^2 = 6\text{-}F$, $R^3 = R^4 = R^5 = OMe$
j: $R^1 = 3'OMePh$, $R^2 = 6,7\text{-}OCH_2O\text{-}$, $R^3 = R^5 = H$, $R^4 = OMe$
k: $R^1 = 3'OMePh$, $R^2 = 6\text{-}C_4H_8N$, $R^3 = R^5 = H$, $R^4 = OMe$
l: $R^1 = 2'FPh$, $R^2 = 6\text{-}C_4H_8N$, $R^3 = R^5 = H$, $R^4 = OMe$
m: $R^1 = Ph$, $R^2 = R^3 = R^5 = H$, $R^4 = NO_2$
n: $R^1 = R^2 = R^3 = R^5 = H$, $R^4 = NO_2$

Scheme 1. *Reagents and conditions*: a) $NaNO_2$/HCl-AcOH, CH_3CN, 0 °C, 30 min; b) SO_2 in AcOH/CuCl, 2 h; c) Anhyd. DMF/K_2CO_3, 2 h.

Results and Discussion

Chemistry

The general method for the synthesis of 2-substituted-quinolin-4-yl-benzenesulfonates **10a**–**n** is outlined in Scheme 1. 4-Methoxybenzenesulfonyl chloride (**12b**), 4-nitrobenzenesulfonyl chloride (**12c**), 4-hydroxyquinoline (**13a**), and 2-methyl-4-hydroxyquinoline (**13b**) are commercially available. 3,4,5-Trimethoxybenzenesulfonyl chloride (**12a**)[33] and 2-substituted-4-hydroxyquinolines (**13b**–**m**) were prepared following the previously described methods.[28–30] The desired sulfonates (**10a**–**n**) were prepared in good yield by combining 2-substituted-4-hydroxyquinolines **13a**–**n** with the appropriate benzenesulfonyl chlorides (**12a**–**c**) in the presence of potassium carbonate in anhydrous DMF.

Biological results

In vitro cytotoxicity

The antiproliferative activities of the newly synthesized sulfonate derivatives (**10a**–**n**) against human lymphoblastic leukemia (CCRF-CEM) and human solid tumor cell growth in culture are summarized in Table 1. Conclusions were made regarding the SAR for these analogues, based on the IC_{50} value of each

Table 1. Cytotoxicity of 2-substituted quinoline-4-yl-benzenesulfonates (**10a**–**n**) in CCRF-CEM, the vinblastine- and taxol-resistant sub-cell lines, and various human solid tumor cell lines.

	IC_{50} [μM][a]							
Compd	CCRF-CEM	CCRF-CEM/VBL[b]	CCRF-CEM/Taxol[b]	HCT-116	HeLa-S3	H460	HT29	PC3
10a	ND[d]	ND	ND	ND	9.32 ± 0.06	ND	ND	ND
10b	2.98 ± 0.44	4.26 ± 0.01 [1.4×][c]	5.12 ± 0.001 [1.7×][c]	3.43 ± 0.06	8.53 ± 0.05	ND	ND	ND
10c	2.34 ± 0.002	6.27 ± 0.40 [2.7×]	3.55 ± 0.05 [1.5×]	5.20 ± 0.16	1.88 ± 0.04	6.80 ± 0.06	4.41 ± 0.03	5.42 ± 0.03
10d	2.39 ± 0.002	3.96 ± 0.07 [1.7×]	3.87 ± 0.04 [1.6×]	4.34 ± 0.02	3.35 ± 0.07	11.54 ± 0.06	7.84 ± 0.15	8.75 ± 0.06
10e	2.00 ± 0.01	5.24 ± 0.01 [2.6×]	3.28 ± 0.14 [1.6×]	5.35 ± 0.07	1.05 ± 0.04	3.11 ± 0.04	2.60 ± 0.04	3.40 ± 0.03
10f	0.28 ± 0.001	1.17 ± 0.11 [4.2×]	1.28 ± 0.01 [4.6×]	0.83 ± 0.003	0.26 ± 0.03	0.34 ± 0.03	0.43 ± 0.09	0.51 ± 0.06
10g	0.75 ± 0.07	1.32 ± 0.004 [1.8×]	1.13 ± 0.04 [1.5×]	1.25 ± 0.01	0.31 ± 0.04	0.58 ± 0.04	0.60 ± 0.09	0.59 ± 0.06
10h	0.38 ± 0.01	0.99 ± 0.01 [2.5×]	0.59 ± 0.02 [1.5×]	1.07 ± 0.03	0.64 ± 0.05	2.47 ± 0.06	3.07 ± 0.02	1.50 ± 0.08
10i	0.50 ± 0.02	1.28 ± 0.01 [2.6×]	1.04 ± 0.01 [2.1×]	1.17 ± 0.001	1.21 ± 0.05	ND	ND	ND
10j	1.80 ± 0.06	8.46 ± 0.05 [4.7×]	3.98 ± 0.11 [2.2×]	6.39 ± 0.09	1.84 ± 0.04	6.26 ± 0.05	4.00 ± 0.20	4.07 ± 0.06
10k	0.81 ± 0.01	1.67 ± 0.002 [2.1×]	1.05 ± 0.01 [1.3×]	0.99 ± 0.01	0.37 ± 0.04	0.44 ± 0.04	0.77 ± 0.09	0.68 ± 0.05
10l	1.46 ± 0.02	2.63 ± 0.01 [1.8×]	2.31 ± 0.02 [1.6×]	3.12 ± 0.04	0.31 ± 0.03	0.47 ± 0.04	0.66 ± 0.07	0.64 ± 0.05
10m	0.47 ± 0.001	1.70 ± 0.04 [3.6×]	0.91 ± 0.04 [1.9×]	1.34 ± 0.02	0.33 ± 0.03	0.79 ± 0.06	0.90 ± 0.07	0.79 ± 0.04
10n	ND	ND	ND	ND	> 100	ND	ND	ND
vinblastine	0.0007 ± 0.0001	0.50 ± 0.12 [680×]	0.08 ± 0.01 [106×]	ND	0.0006 ± 0.00003	0.0014 ± 0.0004	0.002 ± 0.0001	0.001 ± 0.0001
taxol	0.0012 ± 0.0001	1.27 ± 0.05 [980×]	0.43 ± 0.04 [358×]	ND	0.003 ± 0.00001	0.004 ± 0.00002	0.006 ± 0.0001	0.004 ± 0.0001

[a] Data represent the mean ± SD of each compound from three to six independent experiments. [b] CCRF-CEM/VBL and CCRF-CEM/Taxol are sub-cell lines of CCRF-CEM cells with 680-fold resistance to vinblastine and 358-fold resistance to taxol, respectively, relative to the IC_{50} value of the parent cell line. [c] Numbers in brackets are measures of cross-resistance as determined by comparison with the corresponding IC_{50} value of the parent cell line. [d] Not determined.

compound in CCRF/CEM cells. Within the series of 3,4,5-trimethoxyphenyl sulfonate derivatives (**10a–i**), the 2-substututed phenyl derivatives (**10c–i**, IC_{50} = 0.28–2.39 μM) are more cytotoxic than the C2-unsubstituted compound (**10a**, IC_{50} = 9.32 μM) and 2-methyl-substituted compound (**10b**, IC_{50} = 2.98 μM). The 6,7-methylenedioxy-2-phenylquinoline derivatives (**10c–e**) can be ranked in the following order with respect to potency: 2[2′-fluorophenyl] (**10e**) > 2-phenyl (**10c**) > 2[3′-methoxyphenyl] (**10d**). However, 2[3′-methoxyphenyl] derivative **10f** is more cytotoxic than 2[2′-fluorophenyl] **10g** among the 6-pyrrolidinyl quinolines. Additionally, among the series of 3′-methoxyphenyl derivatives, 6-chloroquinoline derivative **10h** exhibits greater cytotoxicity than the corresponding 6-fluoroquinoline derivative (**10i**).

The 4-methoxyphenyl sulfonate derivative series (**10j–l**) can be ranked in order of decreasing potency as follows: **10k** > **10l** > **10j**. The 4′-nitrophenyl sulfonate (**10m**) was one of the most potent derivatives, with an IC_{50} value of 0.47 μM against CCRF/CEM cell growth in culture. It should be noted that 2-[2′-fluorophenyl]-6-pyrrolinylquinoline derivatives exhibit significant cytotoxicity with both 3′,4′,5′-trimethoxyphenyl (**10f**, and **10g**) and 4-methoxyphenyl sulfonates (**10k** and **10l**). We further evaluated the cytotoxicity of the newly synthesized sulfonates in human solid tumor cell lines (HCT-116, HeLa-S3, H460, HT29, and PC3). Compounds **10f**, **10g**, **10k**, and **10m** exhibited a broad spectrum of antitumor activity, with IC_{50} values ranging from 0.28–1.34 μM against the cell lines tested. It should be noted that compounds without a C2 substituent, **10a** and **10n**, exhibit less or no cytotoxicity, respectively, than the other compounds, indicating the importance of a substituent at the C2 position.

One major limitation of anticancer drugs is acquired multidrug resistance (MDR). We used CCRF/CEM cells, the vinblastine-resistant subline (CCRF-CEM/VBL, 680-fold resistance to

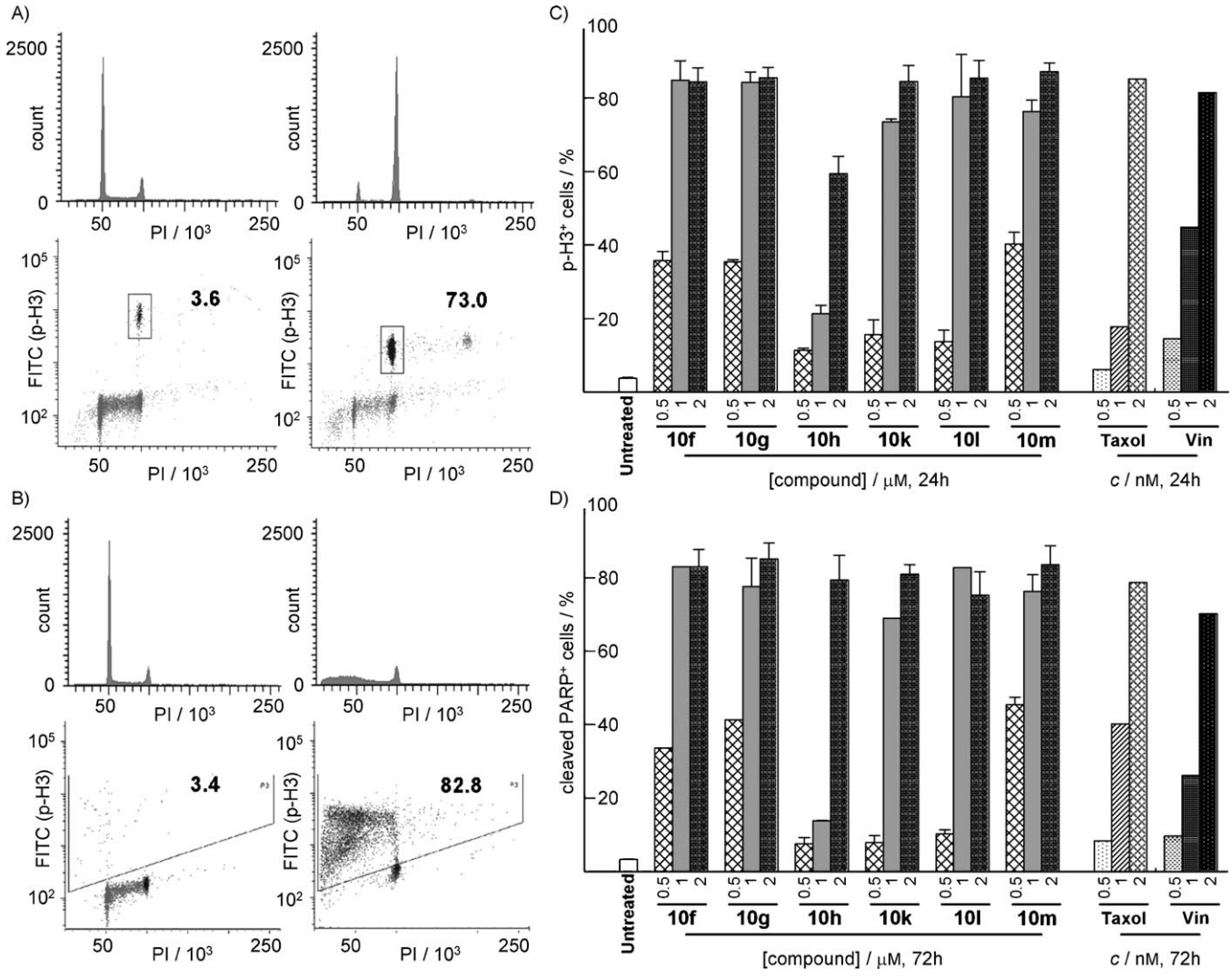

Figure 2. A) and B) Quinoline sulfonates induce mitotic arrest and apoptosis: Representative flow cytometry data for untreated and compound **10m**-treated (1 μM for 24 or 72 h) cells stained with PI for DNA labeling and with an antibody against phospho-histone H3 (p-H3) to label mitotic cells (A) or with an antibody against cleaved PARP to label apoptotic cells (B). Rectangles indicate p-H3-positive or cleaved PARP-positive cells; the percentage of mitotic or apoptotic cells is indicated in bold. C) and D) Quinoline sulfonates induce accumulation of mitotic cells: HeLa-S3 cells were treated with 0.5–2 μM quinoline sulfonates or 0.5–2 nM taxol or vinblastine (Vin) for 24 (C) and 72 h (D), then cell cycle distribution (C) and apoptosis (D) were analyzed as described in the Experimental Section. Data are the mean ±SD of four independent experiments.

vinblastine in vitro), and the taxol-resistant subline (CCRF-CEM/taxol, 358-fold resistance to taxol in vitro) to evaluate whether the compounds could overcome the MDR developed in these sublines (Table 1). The resulting IC_{50} values showed that the sulfonates are 1.4- to 4.7-fold less cytotoxic in the resistant sublines than in parent CCRF/CEM cells. This indicates that the tested sulfonates have little or no cross-resistance to vinblastine or taxol and are not good substrates for membrane MDR transporters.

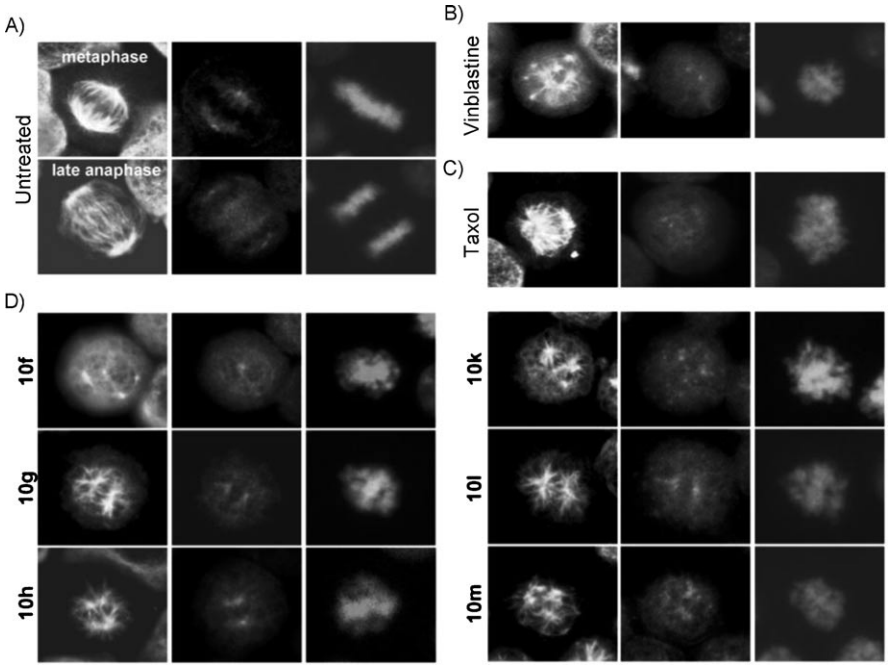

Figure 3. Quinoline sulfonates induce abnormal mitotic spindles: Representative immunofluorescence images showing abnormal spindles in mitotic cells arrested by quinoline sulfonates, taxol, or vinblastine. HeLa-S3 cells seeded on glass cover slips were treated for 14 h with A) vehicle, B) 10 nM vinblastine, C) 10 nM taxol, or D) 1 μM quinoline sulfonates, and stained with an anti-α-tubulin antibody to detect mitotic spindles (left), with an anti-γ-tubulin antibody to detect centrosomes (center), and with DAPI to detect chromosomes (right).

Induction of mitotic arrest and apoptosis

Six of the compounds exhibiting the highest levels of cytotoxicity in regard to inhibition of cancer cell growth (**10f**, **10g**, **10h**, **10k**, **10l**, and **10m**) were examined for their effects on cell cycle progression and apoptosis induction in HeLa-S3 cells by flow cytometry analysis of phospho-histone H3 (a mitosis marker) and cleaved poly(ADP-ribose) polymerase (PARP; an apoptosis marker). Results showed that drug treatment induced a significant increase in mitotic cells at 24 h (Figure 2A and C) and apoptosis at 72 h (Figure 2B and D), indicating that cells were first arrested at mitosis and then underwent apoptosis following treatment with sulfonate derivatives. Of the compounds tested, **10h**, which exhibits relatively low cytotoxicity ($IC_{50} = 0.64$ μM in HeLa-S3 cells), induced low levels of mitotic arrest and apoptosis at 0.5 and 1 μM, respectively. The other compounds (**10f**, **10g**, **10k**, **10l**, and **10m**) have higher cytotoxicity (IC_{50}: 0.26–0.37 μM in HeLa-S3 cells) and induced higher levels of mitotic arrest and apoptosis at the same concentrations. These results indicate that the ability of these drugs to induce mitotic arrest and apoptosis correlate well with their antiproliferative activities.

Antimitotic effects of sulfonates

As selected sulfonates (1–2 μM concentration) induced nearly 80% of cells arrested at mitosis 24 h after treatment (Figure 2C), their effects on mitotic spindles were evaluated. The results showed that the bipolar spindles are organized in an oval shape, while the chromosomes are aligned at metaphase plates in all metaphases from untreated HeLa-S3 cells (Figure 3A). In contrast, all of the mitotic cells arrested using 1 μM of the tested compounds (**10f**, **10g**, **10h**, **10k**, **10l**, and **10m**) contained highly abnormal mitotic spindles with multiple

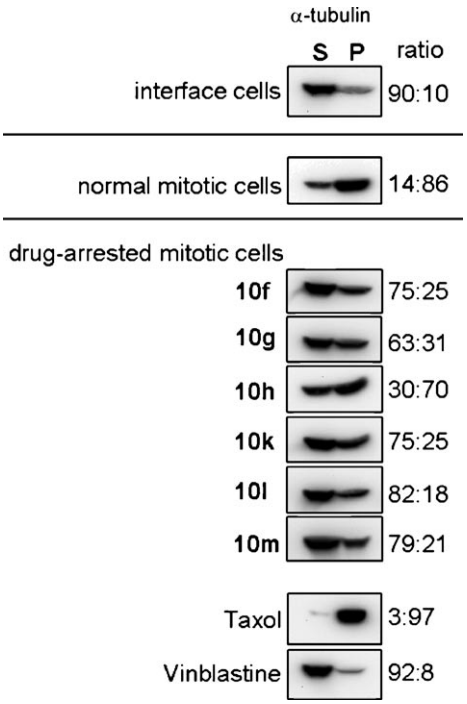

Figure 4. Quinoline sulfonates inhibit cellular tubulin polymerization: HeLa-S3 cells were treated with 1 μM sulfonates, 10 nM vinblastine, or 10 nM taxol for 24 h. Mitotic cells were removed by shaking, and equal amounts of cells were lysed and analyzed as described in the Experimental Section. S, soluble α-tubulin; P, polymerized α-tubulin. Ratios to the right of each blot indicate percentage of polymerized or soluble tubulin as determined by dividing the densitometric value for each tubulin fraction by the total tubulin content (polymerized + soluble tubulin). Normal mitotic cells were obtained from cultures released after 10 h from a double-thymidine block.

poles, shortened and dispersed microtubule fibers, and mis-segregated chromosomes (Figure 3D). This pattern is similar to that shown for vinblastine-arrested mitotic cells (Figure 3B), and indicates that the sulfonate derivatives disrupt the assembly of bipolar spindles and alter chromosome segregation, inducing mitotic arrest and apoptosis.

To ascertain the mechanism of action for the sulfonates, we evaluated their effects on cellular microtubules using the cellular microtubule stabilization assay. The results showed that tubulin extracted from synchronized mitotic cells is primarily in the polymerized form (Figure 4). In contrast, up to 80% of tubulin extracted from sulfonate-arrested mitotic cells is in the soluble form, as observed in vinblastine-arrested mitotic cells. Tubulin extracted from taxol-arrested mitotic cells is primarily polymerized. Therefore, taxol stabilizes and vinblastine destabilizes tubulin polymerization, as expected, while the sulfonates inhibit cellular tubulin polymerization.

Interaction of sulfonates with tubulin and targeting of the vinblastine binding site

A majority of compounds that inhibit tubulin polymerization bind to tubulin at either the colchicine site or the vinblastine site.[6] Therefore, through competitive binding assays, we examined whether or not sulfonate derivatives interact with tubulin directly by binding to these sites. The binding of sulfonates to tubulin was first investigated by measuring the effects of these drugs on the intrinsic tryptophan fluorescence of tubulin. Compound **10h** was not included because it has strong auto fluorescence, which interferes with measurement. As shown in Figure 5A, all of the sulfonate derivatives evaluated (**10f**, **10g**, **10k**, **10l**, and **10m**) decrease the intrinsic tryptophan fluorescence of tubulin similarly to vinblastine, indicating that these drugs interact with tubulin. The intrinsic fluorescence of colchicine increases upon binding to tubulin,[34] which was used as an indicator for the competition of sulfonate derivatives with colchicine in tubulin binding. Our results showed that pre-incubation of tubulin with each sulfonate derivative does not decrease the fluorescence of the colchicine–tubulin complex (Figure 5B), indicating that these agents have no effect on the colchicine–tubulin interaction. In contrast, pre-incubation of tubulin with colcemid, a colchicine analogue with very low fluorescence upon binding to tubulin,[35] significantly decreased fluorescence of the colchicine–tubulin complex. These results indicate that the tubulin binding site of these sulfonate derivatives is different from that of colchicine.

The fluorescence of BODIPY FL-vinblastine, a fluorescent derivative of vinblastine, increases significantly upon binding to tubulin.[36] Therefore, BODIPY FL-vinblastine was employed to detect whether the tested sulfonate derivatives could bind to the vinblastine binding site. Pre-incubation of tubulin with each of the sulfonate derivatives or vinblastine significantly decreases the fluorescence of BODIPY FL-vinblastine (Figure 5C), indicating that these agents prevent the binding of BODIPY FL-vinblastine to tubulin. Taxol, by comparison, which does not bind to the vinblastine binding site of tubulin, has no effect on the fluorescence of BODIPY FL-vinblastine. Compound **10a**, which exhibits relatively low cytotoxicity in HeLa-S3 cells, has no effect on the intrinsic tryptophan fluorescence of tubulin (Figure 5A) and does not compete for the vinblastine binding site of tubulin as the other sulfonate derivatives do (Figure 5C). These findings provide evidence that the newly synthesized sulfonate derivatives interact directly with tubulin through the vinblastine site but not the colchicine site. Additionally, the results suggest that the affinity of drug–tubulin binding may not have correlate directly with drug cytotoxicity.

Conclusions

We have synthesized a series of 2-substituted quinolin-4-yl-benzenesulfonates for evaluation of in vitro cytotoxicity. Of these derivatives, compounds with a 6-pyrrolidinyl functionality (e.g., **10f**, **10g**, and **10k**) and 4′-nitrophenyl sulfonate (**10m**) exhibit significant antiproliferative activities against all tumor cell lines tested. We found that these sulfonates are able to induce a significant increase in mitotic arrest and apoptosis. Studies regarding the effects of these compounds on mitotic spindles revealed that the synthesized sulfonates interfere with assembly and function of mitotic spindles and block mitosis progression, thereby inducing apoptosis. Previous studies showed that sulfonate analogues of CA-4 bind to the colchicine binding domain of tubulin.[26] In contrast, the compounds synthesized in this study bind to the vinblastine, but not the colchicines, domain. Among known tubulin polymerization inhibitors, vinblastine and colchicine binding sites, as well as their mechanisms of action of these compound, have been studied thoroughly. As mentioned previously, colchicine derivatives have limited applications in cancer chemotherapy due to their toxicity, which results in hemorrhaging and necrosis.[37] Most drugs that interact with tubulin are isolated from natural products (e.g., vinca alkaloids and related analogues); only a few inhibitors are derived from synthetic compounds.[38,39] Although vinca alkaloids and taxol analogues are important categories of antimitotic drugs, both rapidly develop MDR due to overexpression of P-glycoprotein or mutated tubulin, which decreases their therapeutic efficacy. The newly synthesized sulfonates, however, have no cross-resistance to the MDR cell lines evaluated, suggesting that it may be possible to optimize the antitumor efficacy of these sulfonates via structural modification to generate more promising antitubulin agents for clinical application.

Experimental Section

Chemistry: general methods

All commercial chemicals and solvents were reagent grade and were used without further purification unless otherwise specified. Melting points were determined using a Fargo melting point apparatus and are uncorrected. Column chromatography was carried out on silica gel G60 (70–230 mesh, ASTM, Merck; and 230–400 mesh, Silicycle Inc.). All high-resolution mass spectra were recorded using a Bruker BioTOF II mass spectrometer using ESI in positive ion mode. Thin-layer chromatography was performed on silica gel G60 F_{254} (Merck) with short-wavelength UV light for visualization.

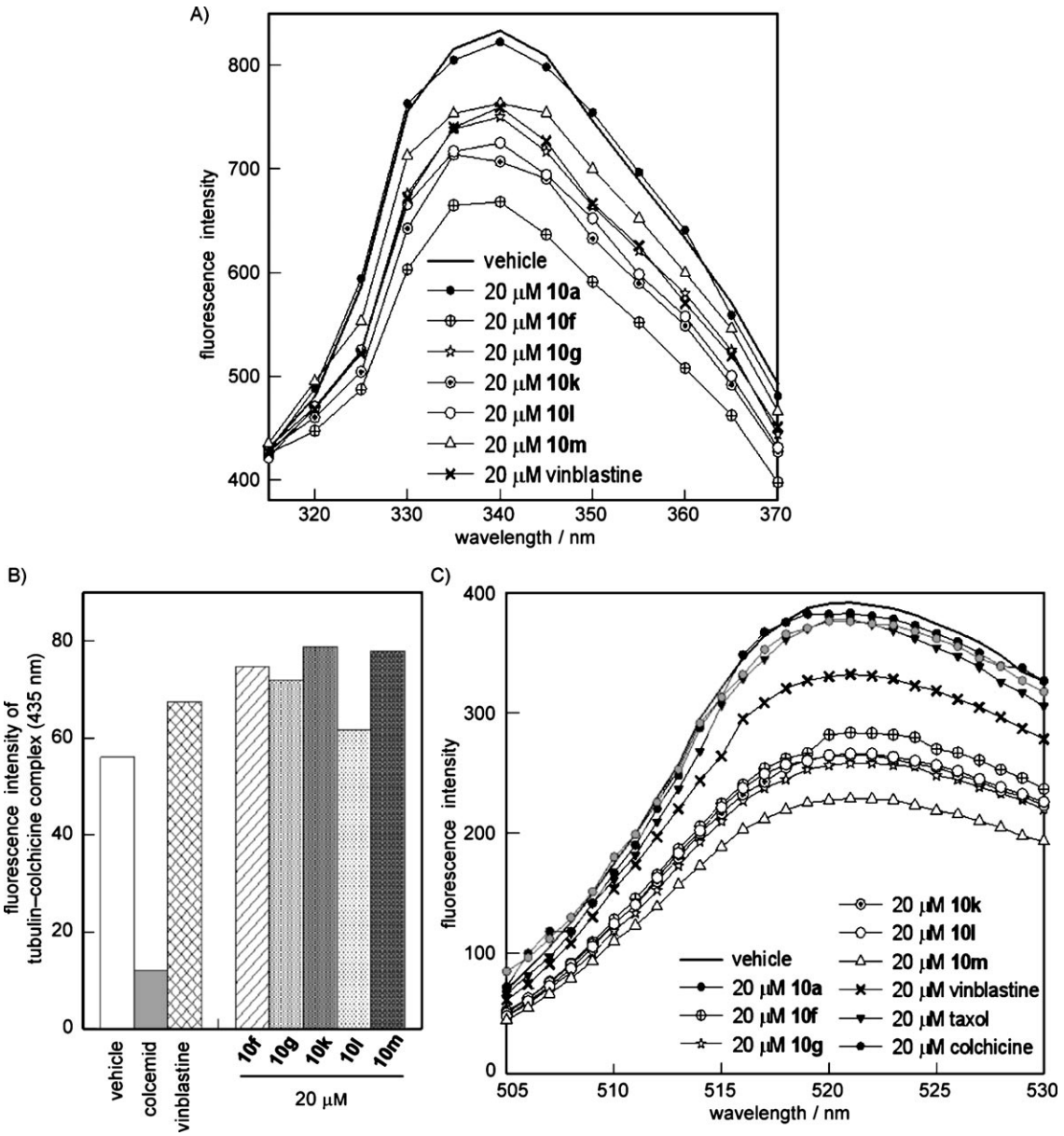

Figure 5. Characterization of binding of quinoline sulfonates to tubulin: A) Quinoline sulfonates decrease the intrinsic tryptophan fluorescence of tubulin. The excitation wavelength was 295 nm, and one of four experiments is shown. B) Quinoline sulfonates do not alter fluorescence of the tubulin–colchicine complex. Tubulin (5 μM) was first incubated with 20 μM each quinoline sulfonate, 20 μM colcemid, or 20 μM vinblastine at 37 °C for 45 min, then 20 μM colchicine was added to each of the mixtures. Fluorescence was measured after incubation for 20 min at 37 °C. Excitation and emission wavelengths were 350 and 435 nm, respectively. Data are the average of two independent experiments. C) Quinoline sulfonates inhibit binding of vinblastine to tubulin. Tubulin (3 μM) was first incubated with 20 μM quinoline sulfonates, 20 μM taxol, or 20 μM vinblastine at 37 °C for 45 min, then 3 μM BODIPY FL-vinblastine was added to each of the mixtures. Fluorescence was measured after incubation for 20 min at 37 °C. The excitation wavelength was 490 nm, and one of four experiments is shown.

All reported yields correspond to isolated yields after chromatography or crystallization. Elemental analyses were done using a Heraeus CHN-O Rapid instrument. ^{1}H NMR and ^{13}C NMR spectra were recorded on a 600 MHz, Brucker AVANCE 600 DRX and 400 MHz, Brucker Top-Spin spectrometers in the solvents indicated. Chemical shifts (δ) are reported in ppm relative to $(CH_3)_4Si$. High-performance liquid chromatography (HPLC) purity analyses of synthesized compounds were recorded on a Hitachi D-2000 Elite instrument with a Mightysil RP-18 GP 250–4.6 column (5 μm); mobile phase: 90% CH_3CN, 5% THF, and 5% H_2O over 25 min or 90% CH_3CN and 10% MeOH over 25 min; flow rate: 1 mL min^{-1}; injected sample volume: 10 μL; column $T = 27$ °C; $\lambda = 254$ nm. The purity of all compounds was ≥ 95% based on two analytical HPLC methods.

Starting materials for preparing 2-substituted-quinolin-4-yl-benzenesulfonates: 4-methoxybenzenesulfonyl chloride (**12b**), 4-nitrosulfonyl chloride (**12c**), quinolin-4(1*H*)-one (**13a**), and 2-methylquinolin-4(1*H*)-one (**13b**) are commercially available; 3,4,5-trimethoxyphenylsulfonyl chloride (**12a**) was prepared as previously described.[33] 2-Substituted 4-hydroxyquinolines were prepared following methods described in literature.[28–30]

Quinolin-4-yl-3,4,5-trimethoxybenzenesulfonate (10a): Potassium carbonate (0.55 g, 4 mmol) was added to a solution of quinolin-4(1*H*)-one **13a** (0.29 g, 2 mmol) in anhydrous DMF (10 mL). The mixture was sonicated for 20 min, then cooled to 0 °C. A solution of 3,4,5-trimethoxybenzenesulfonyl chloride (**12a**, 0.69 g, 4 mmol) in anhydrous DMF (5 mL) was added dropwise. The resulting solution was stirred at room temperature for 2 h. The solvent was evaporated to dryness in vacuo, and the residue was dissolved in CH_2Cl_2 and washed with H_2O. The organic phases were combined, dried over anhydrous Na_2SO_4, filtered, and evaporated in vacuo. The resulting crude solid was recrystallized from EtOH to give **10a**. Yield, 0.67 g (89%); mp: 93–94 °C; ^{1}H NMR ([D$_6$]DMSO): δ = 3.73 (s, 3H, OMe), 3.77 (s, 6H, 2×OMe), 7.16 (s, 2H, 2×ArH), 7.45 (d, 1H, J = 4.5 Hz, ArH), 7.62 (t, 1H, J = 7.6 Hz, ArH), 7.82 (t, 1H, J = 7.6 Hz, ArH), 7.90 ppm (d, 1H, J = 8.4 Hz, ArH); ^{13}C NMR (400 MHz, [D$_6$]DMSO): δ = 56.46, 60.37, 105.88, 113.15, 121.30, 121.66, 127.55, 128.23, 128.93, 130.62, 143.00, 148.47, 151.39, 152.22, 153.18 ppm; HRMS calcd for $C_{18}H_{17}NO_6S$: 376.0856 $[M+H]^+$, found: 376.2784; MS (EI) *m/z* (rel. intensity): 375.0 (29%) $[M]^+$.

*The following compounds were prepared using the same synthetic method as for **10a**:*

2-Methylquinolin-4-yl-3,4,5-trimethoxybenzenesulfonate (10b): Compound **10b** was prepared from 2-methylquinolin-4(1*H*)-one (**13b**, 0.41 g, 2.56 mmol) and **12a** (0.80 g, 3 mmol). Yield: 0.80 g, 80%; mp: 99–101 °C; ^{1}H NMR ([D$_6$]DMSO): δ = 2.67 (s, 3H, Me), 3.67–3.84 (m, 9H, 3×OMe), 7.11–7.19 (m, 2H, ArH), 7.33 (s, 1H, ArH), 7.47–7.52 (m, 1H, ArH), 7.68–7.86 (m, 2H, ArH), 7.89–8.04 ppm (m, 1H, ArH); ^{13}C NMR ([D$_6$]DMSO): δ = 24.65, 56.49, 60.35, 102.94, 105.97, 113.71, 120.06, 121.20, 123.56, 126.72, 128.19, 130.83, 143.08, 151.96, 153.16, 159.97 ppm; HRMS $[M+H]^+$ calcd for $C_{19}H_{19}NO_6S$: 390.1011, found: 390.2993; MS (EI) *m/z* $[M]^+$ (rel. intensity): 388.9 (17%); Anal. calcd for $C_{19}H_{19}NO_6S$: C 58.60, H 4.92, N 3.60, S 8.23, found: C 58.57, H 4.70, N 3.62, S 8.57.

6-Phenyl-[1,3]dioxolo[4,5-*g*]quinolin-8-yl-3,4,5-trimethoxybenzenesulfonate (10c): Compound **10c** was prepared from 6-phenyl-[1,3]dioxolo[4,5-*g*]quinolin-8(5*H*)-one (**13c**, 0.80 g, 3 mmol) and **12a** (1.20 g, 4.5 mmol). Yield: 1.09 g, 74%; mp: 142–143 °C; ^{1}H NMR ([D$_6$]DMSO): δ = 3.74 (s, 3H, OMe), 3.75 (s, 6H, 2×OMe), 6.23 (s, 2H, CH_2), 7.12 (s, 1H, ArH), 7.19 (s, 2H, 2×ArH), 7.45 (s, 1H, ArH), 7.55–7.49 (m, 3H, 3×ArH), 7.64 (s, 1H, ArH), 8.08–8.06 ppm (m, 1H, ArH); ^{13}C NMR ([D$_6$]DMSO): δ = 56.46, 60.33, 96.48, 102.55, 105.24, 106.22, 109.36, 117.60, 126.68, 127.14, 128.18, 128.67, 128.80, 129.64, 137.73, 143.14, 147.93, 148.41, 151.58, 152.49, 153.18, 154.69 ppm; HRMS $[M+H]^+$ calcd for $C_{25}H_{21}NO_8S$: 496.1066, found: 496.3615; MS (EI) *m/z* $[M]^+$ (rel. intensity): 495.0 (39%); Anal. calcd for $C_{25}H_{21}NO_8S$: C 60.60, H 4.27, N 2.83, S 6.47, found: C 60.52, H 4.04, N 3.12, S 6.52.

6-(3-Methoxyphenyl)-[1,3]dioxolo[4,5-*g*]quinolin-8-yl-3,4,5-trimethoxybenzenesulfonate (10d): Compound **10d** was prepared from 6-(3-methoxyphenyl)-[1,3]dioxolo[4,5-*g*]quinolin-8(5*H*)-one (**13d**, 1.47 g, 5 mmol) and **12a** (2.00 g, 7.5 mmol). Yield: 2.10 g, 81%; mp: 151–152 °C; ^{1}H NMR ([D$_6$]DMSO): δ = 3.74 (s, 3H, OMe), 3.76 (s, 6H, 2×OMe), 3.85 (s, 3H, OMe), 6.20 (s, 2H, CH_2), 7.06–7.08 (m, 1H, ArH), 7.13 (s, 1H, ArH), 7.18 (s, 2H, 2×ArH), 7.42–7.45 (m, 2H, 2×ArH), 7.62–7.63 ppm (m, 3H, 3×ArH); ^{13}C NMR ([D$_6$]DMSO): δ = 55.19, 56.47,60.33, 96.52, 102.58, 105.29, 106.22, 109.65, 111.98, 115.35, 117.77, 119.05, 128.18, 129.93, 139.20, 143.13, 147.86, 148.49, 151.62, 152.48, 153.19, 154.47, 159.73 ppm; HRMS $[M+H]^+$ calcd for $C_{26}H_{23}NO_9S$: 526.1172, found: 526.3872; MS (EI) *m/z* $[M]^+$ (rel. intensity): 525.1 (17%); Anal. calcd for $C_{26}H_{23}NO_9S$: C 59.42, H 4.41, N 2.67, S 6.10, found: C 59.64, H 4.36, N 2.98, S 6.25.

6-(2-Fluorophenyl)-[1,3]dioxolo[4,5-*g*]quinolin-8-yl-3,4,5-trimethoxybenzenesulfonate (10e): Compound **10e** was prepared from 6-(2-fluorophenyl)-[1,3]dioxolo[4,5-*g*]quinolin-8(5*H*)-one (**13e**, 1.13 g, 4 mmol) and **12a** (1.60 g, 6 mmol). Yield: 1.87 g, 89%; mp: 176–177 °C; ^{1}H NMR ([D$_6$]DMSO): δ = 3.72 (s, 3H, OMe), 3.77 (s, 6H, 2×OMe), 6.26 (s, 2H, CH_2), 7.20 (s, 2H, 2×ArH), 7.22 (s, 1H, ArH), 7.32–7.39 (2H, m 2×ArH), 7.46 (s, 1H, ArH), 7.47 (s, 1H, ArH), 7.52–7.55 (m, 1H, ArH), 8.01–8.05 ppm (m, 1H, ArH); ^{13}C NMR ([D$_6$]DMSO): δ = 56.43, 60.32, 96.44, 102.72, 105.27, 106.09, 112.35, 116.49, 117.66, 124.90, 125.95, 128.13, 130.85, 131.62, 143.08, 147.96, 148.87, 150.95, 151.84, 153.21, 158.71, 161.19 ppm; HRMS $[M+H]^+$ calcd for $C_{25}H_{20}FNO_8S$: 514.0972, found: 514.3616; MS (EI) *m/z* $[M^+]$ (rel. intensity): 513.0 (18%); Anal. calcd for $C_{25}H_{20}FNO_8S$: C 58.48, H 3.93, N 2.73, S 6.24, found: C 58.28, H 4.03, N 3.04, S 6.56.

2-(3-Methoxyphenyl)-6-(pyrrolidin-1-yl)quinolin-4-yl-3,4,5-trimethoxybenzenesulfonate (10f): Compound **10f** was prepared from 2-(3-methoxyphenyl)-6-(pyrrolidin-1-yl)quinolin-4(1*H*)-one (**13f**, 0.80 g, 2.5 mmol) and **12a** (0.94 g, 3.5 mmol). Yield: 1.18 g, 85%; mp: 168–169 °C; ^{1}H NMR ([D$_6$]DMSO): δ = 1.98 (m, 4H, 2×CH_2), 3.24 (m, 4H, 2×CH_2), 3.69 s, 9H, 3×OMe), 3.86 (s, 3H, OMe), 6.33–6.32 (m, 1H, ArH), 7.04–7.02 (m, 1H, ArH), 7.10 (s, 2H, 2×ArH), 7.29–7.26 (m, 1H, ArH), 7.44–7.40 (m, 1H, ArH), 7.66–7.64 (m, 2H, 2×ArH), 7.71 (s, 1H, ArH), 7.91–7.89 ppm (m, 1H, ArH); ^{13}C NMR ([D$_6$]DMSO): δ = 24.93, 47.29, 55.17, 56.29, 60.22, 95.76, 105.86, 111.54, 114.80, 118.72, 120.40, 122.84, 128.89, 129.86, 130.11, 130.85, 139.68, 142.93, 145.88, 150.56, 151.13, 153.18, 159.74, 160.89 ppm; HRMS $[M+H]^+$ calcd for $C_{29}H_{30}N_2O_7S$: 551.1851, found: 551.4715; MS (EI) *m/z* $[M]^+$ (rel. intensity): 550.2 (14%); Anal. calcd for $C_{29}H_{30}N_2O_7S$: C 63.26, H 5.49, N 5.09, S 5.82, found: C 63.25, H 5.46, N 5.26, S 6.13.

2-(2-Fluorophenyl)-6-(pyrrolidin-1-yl)quinolin-4-yl-3,4,5-trimethoxybenzenesulfonate (10g): Compound **10g** was prepared from 2-(2-fluorophenyl)-6-(pyrrolidin-1-yl)quinolin-4(1*H*)-one (**13g**, 0.90 g, 3.0 mmol) and **12a** (1.20 g, 4.5 mmol). Yield: 1.23 g, 76%; mp: 174–175 °C; ^{1}H NMR ([D$_6$]DMSO): δ = 1.99, (m, 4H, 2×CH_2), 3.28, (m, 4H, 2×CH_2), 3.69, (s, 3H, OMe), 3.71, (s, 6H, 2×OMe), 6.38–6.39, (m, 1H, ArH), 7.13, (s, 2H, 2×ArH), 7.30–7.38, (m, 3H, 3×ArH), 7.48–7.53, (m, 1H, ArH), 7.56, (s, 1H, ArH), 7.90–7.92, (m, 1H, ArH), 8.04–8.08 ppm (m, 1H, ArH); ^{13}C NMR ([D$_6$]DMSO): δ = 24.90, 47.30, 56.24, 60.19, 95.48, 105.79, 114.23, 116.18, 120.52, 122.71, 124.78, 126.44, 128.75, 130.12, 130.60, 130.93, 142.96, 146.10, 146.94, 150.34, 153.16, 158.64, 161.11 ppm; HRMS $[M+H]^+$ calcd for $C_{28}H_{27}FN_2O_6S$: 539.1652, found: 539.4455; MS (EI) *m/z* $[M]^+$ (rel. intensity): 538.1 (8%); Anal. calcd for $C_{28}H_{27}FN_2O_6S$: C 62.44, H 5.05, N 5.20, S 5.95, found: C 62.16, H 4.90, N 5.32, S 5.92.

6-Chloro-2-(3-methoxyphenyl)quinolin-4-yl-3,4,5-trimethoxybenzenesulfonate (10h): Compound **10h** was prepared from 6-chloro-2-(3-methoxyphenyl)quinolin-4(1*H*)-one (**13h**, 1.01 g, 3.54 mmol) and **12a** (1.41 g, 5.3 mmol). Yield: 1.20 g, 72%; mp: 132–133 °C; ^{1}H NMR ([D$_6$]DMSO): δ = 3.72 (s, 9H, 3×OMe), 3.87 (s, 3H, OMe), 7.13 (m, 3H, ArH), 7.51–7.47 (m, 1H, ArH), 7.72–7.75 (m, 3H, ArH), 7.82 (m, 1H, ArH), 7.89 (s, 1H, ArH), 8.13–8.11 ppm (m, 1H, ArH); ^{13}C NMR ([D$_6$]DMSO): δ = 55.27, 56.46, 60.24, 106.23, 112.38, 112.68, 116.18, 119.58, 120.16, 121.68, 127.78, 130.10, 131.26, 131.50, 131.96, 138.71, 143.30, 147.45, 152.40, 153.22, 157.40, 159.80 ppm; HRMS $[M+H]^+$ calcd for $C_{25}H_{22}ClNO_7S$: 516.0884, found: 516.3555; MS (EI) *m/z* $[M^+]$ (rel. intensity): 515.0 (7%); Anal. calcd for $C_{25}H_{22}ClNO_7S$: C 58.20, H 4.30, N 2.71, S 6.21, found: C 58.20, H 4.44, N 2.80, S 6.46.

6-Fluoro-2-(3-methoxyphenyl)quinolin-4-yl-3,4,5-trimethoxybenzenesulfonate (10i): Compound **10i** was prepared from 6-fluoro-2-(3-methoxyphenyl)quinolin-4(1*H*)-one (**13i**, 0.50 g, 1.75 mmol) and **12a** (0.71 g, 2.65 mmol). Yield: 0.72 g, 78%; mp: 126–128 °C; ^{1}H NMR ([D$_6$]DMSO): δ = 3.68–3.77 (m, 9H, 3×OMe), 3.86 (s, 3H, OMe), 7.07–7.22 (m, 3H, ArH), 7.43–7.56 (m, 2H, ArH), 7.65–7.80 (m, 3H, ArH), 7.92 (s, 1H, ArH), 8.14–8.24 ppm (m, 1H, ArH); ^{13}C NMR ([D$_6$]DMSO): δ = 55.68, 56.15, 60.29, 103.33, 105.19, 106.10, 112.29, 112.54, 114.54, 119.92, 121.61, 122.18, 128.29, 130.43, 131.52, 141.16, 143.29, 144.80, 151.59, 153.18, 159.92, 160.82 ppm; HRMS $[M+H]^+$ calcd for $C_{25}H_{22}FNO_7S$: 500.1180, found: 500.3733; MS (EI) *m/z* $[M]^+$ (rel. intensity): 498.9 (28%); Anal. calcd for $C_{25}H_{22}FNO_7S$: C 60.11, H 4.44, N 2.80, S 6.42, found: C 60.20, H 4.40, N 2.71, S 6.57.

6-(3-Methoxyphenyl)-[1,3]dioxolo[4,5-*g*]quinolin-8-yl-4-methoxybenzenesulfonate (10j): Compound **10j** was prepared from 6-(3-methoxyphenyl)-[1,3]dioxolo[4,5-*g*]quinolin-8(5*H*)-one (**13d**, 1.03 g, 3.5 mmol) and **12b** (1.08 g, 5.25 mmol). Yield: 1.36 g, 87%; mp: 171–172 °C; ^{1}H NMR ([D$_6$]DMSO): δ = 3.85 (s, 3H, OMe), 3.57 (s, 3H, OMe), 6.25 (s, 2H, CH_2), 7.06–7.07 (m, 1H, ArH), 7.11 (s, 1H, ArH), 7.19 (d, 2H, *J* = 8.68 Hz, 2×ArH), 7.46–7.42 (m, 2H, 2×ArH), 7.49 (s, 1H, ArH), 7.53 (s, 1H, ArH), 7.58–7.60 (m, 1H, ArH), 7.96 ppm (d, 2H, *J* = 8.68 Hz, 2×ArH); ^{13}C NMR ([D$_6$]DMSO): δ = 55.22, 56.04, 96.45, 102.64, 105.38, 109.21, 112.00, 115.18, 115.34, 117.71, 119.10, 125.01, 130.00, 131.07, 139.22, 147.93, 148.60, 151.72, 152.42, 154.44, 159.71, 164.53 ppm; HRMS $[M+H]^+$ calcd for $C_{24}H_{19}NO_7S$: 466.0960, found: 466.3345; MS (EI) *m/z* $[M]^+$ (rel. intensity): 465.1 (30%); Anal. calcd for $C_{24}H_{19}NO_7S$: C 61.93, H 4.11, N 3.01, S 6.89, found: C 61.64, H 4.36, N 2.88, S 6.79.

2-(3-Methoxyphenyl)-6-(pyrrolidin-1-yl)quinolin-4-yl-4-methoxybenzenesulfonate (10k): Compound **10k** was prepared from 2-(3-methoxyphenyl)-6-(pyrrolidin-1-yl)quinolin-4(1*H*)-one (**13f**, 0.64 g, 2 mmol) and **12b** (0.62 g, 3 mmol). Yield: 0.76 g, 77%; mp: 119–120 °C; ^{1}H NMR ([D$_6$]DMSO): δ = 1.99 (m, 4H, 2×CH_2), 3.26 (m, 4H, 2×CH_2), 3.85 (s, 3H, OMe), 3.85 (s, 3H, OMe), 6.37 (s, 1H, ArH), 7.02–7.04 (m, 1H, ArH), 7.15–7.17 (m, 2H, 2×ArH), 7.26–7.29 (m, 1H, ArH), 7.41–7.41 (m, 1H, ArH), 7.57–7.62 (m, 3H, 3×ArH), 7.87–7.93 ppm (m, 3H, 3×ArH); ^{13}C NMR ([D$_6$]DMSO): δ = 24.97, 47.35, 55.14, 55.95, 95.94, 110.99, 111.54, 114.73, 115.15, 118.73, 120.44, 122.70, 125.75, 129.85, 130.14, 130.72, 139.69, 142.99, 145.90, 150.49, 151.04, 159.70, 164.33 ppm; HRMS $[M+H]^+$ calcd for $C_{27}H_{26}N_2O_5S$: 491.1641, found: 491.3707; MS (EI) *m/z* $[M]^+$ (rel. intensity): 490.1 (12%); Anal. calcd for $C_{27}H_{26}N_2O_5S$: C 66.10, H 5.34, N 5.71, S 6.54, found: C 66.18, H 5.00, N 5.73, S 6.45.

2-(2-Fluorophenyl)-6-(pyrrolidin-1-yl)quinolin-4-yl-4-methoxybenzenesulfonate (10l): Compound **10l** was prepared from 2-(2-fluorophenyl)-6-(pyrrolidin-1-yl)quinolin-4(1*H*)-one (**13g**, 0.77 g, 2.5 mmol) and **12b** (0.77 g, 3.75 mmol). Yield: 0.92 g, 77%; mp: 175–176 °C; ^{1}H NMR ([D$_6$]DMSO): δ = 2.01 (m, 4H, 2×CH_2), 3.29 (m, 4H, 2×CH_2), 3.84 (s, 3H, OMe), 6.39–6.40 (m, 1H, ArH), 7.15–7.17 (m, 2H, ArH), 7.29–7.38 (m, 3H, 3×ArH), 7.48–7.53 (m, 1H, ArH), 7.56 (s, 1H, ArH), 7.88–7.93 (m, 3H, 3×ArH), 8.04–8.07 ppm (m, 1H, ArH); ^{13}C NMR ([D$_6$]DMSO): δ = 25.03, 47.40, 56.00, 95.61, 113.92, 115.21, 116.29, 120.62, 122.59, 124.88, 125.66, 126.49, 130.22, 130.67, 131.01, 143.14, 146.14, 146.94, 150.32, 158.69, 161.16, 164.38 ppm; HRMS $[M+H]^+$ calcd for $C_{26}H_{23}FN_2O_4S$: 479.1441, found: 479.1382; MS (EI) *m/z* $[M]^+$ (rel. intensity): 478.1 (15%); Anal. calcd for $C_{26}H_{23}FN_2O_4S$: C 65.26, H 4.84, N 5.85, S 6.70, found: C 65.29, H 4.59, N 5.85, S 6.67.

2-Phenylquinolin-4-yl-4-nitrobenzenesulfonate (10m): Compound **10m** was prepared from 2-phenylquinolin-4(1*H*)-one (**13j**, 1.10 g, 5 mmol) and **12c** (1.86 g, 7.0 mmol). Yield: 1.50 g, 82%; mp: 176–177 °C; ^{1}H NMR ([D$_6$]DMSO): δ = 7.56–7.64 (m, 4H, 4×ArH), 7.84–7.86 (m, 2H, 2×ArH), 7.95 (s, 1H, ArH), 8.13–8.15 (m, 1H, ArH), 8.18–8.20 (m, 2H, 2×ArH), 8.35–8.37 (m, 2H, 2×ArH), 8.44–8.46 ppm (m, 2H, 2×ArH); ^{13}C NMR ([D$_6$]DMSO): δ = 110.81, 120.44, 121.02, 123.31, 125.15, 126.90, 127.27, 127.74, 128.22, 128.98, 129.23, 130.31, 131.30, 137.46, 139.15, 149.27, 151.32, 152.88, 157.14 ppm; HRMS $[M+H]^+$ calcd for $C_{21}H_{14}N_2O_5S$: 407.0702, found: 407.2792; MS (EI) *m/z* $[M]^+$ (rel. intensity): 405.9 (38%); Anal. calcd for $C_{21}H_{14}N_2O_5S$: C 62.06, H 3.47, N 6.89, S 7.89, found: C 61.91, H 3.49, N 6.92, S 7.75.

Quinolin-4-yl-4-nitrobenzenesulfonate (10n): Compound **10n** was prepared from quinolin-4(1*H*)-one (**13a**, 0.15 g, 1 mmol) and **12c** (0.33 g, 2 mmol). Yield: 0.29 g, 88%; mp: 233–234 °C; ^{1}H NMR ([D$_6$]DMSO): δ = 7.39 (d, 1H, *J* = 4.92 Hz, ArH), 7.69–7.65 (m, 1H, ArH), 7.88–7.84 (m, 1H, ArH), 7.91 (d, 1H, *J* = 8.3 Hz, ArH), 8.10 (d, 1H, *J* = 8.3 Hz, ArH), 8.33 (d, 2H, *J* = 8.84 Hz, 2×ArH), 8.45 (d, 2H, *J* = 8.84 Hz, 2×ArH), 8.94 (d, 1H, *J* = 4.92 Hz, ArH); ^{13}C NMR (400 MHz, [D$_6$]DMSO): δ = 112.89, 121.05, 121.30, 125.21, 128.0, 129.10, 130.18, 130.89, 139.15, 149.59, 151.33, 151.39, 151.78 ppm; HRMS $[M+H]^+$ calcd for $C_{15}H_{10}N_2O_5S$: 331.0389, found: 331.2077; MS (EI) *m/z* $[M]^+$ (rel. intensity): 330.0 (27%). $[M]^+$.

Cytotoxicity assays

In vitro cytotoxicities of the newly synthesized quinoline sulfonates were determined in T-cell acute lymphocytic leukemia (CCRF-CEM) and its resistant sublines (CCRF-CEM/VBL and CCRF-CEM/taxol) using the XTT assay,[40] and human colon carcinoma (HCT-116) with the SRB assay[41] over a 72 h incubation using a microplate spectrophotometer as previously described.[42] After the addition of phenazine methosulfate–XTT solution, incubated at 37 °C for 6 h, absorbance at 450 and 630 nm was detected using a microplate reader (EL 340). IC_{50} values were determined from dose–effect relationships measured with six or seven concentrations of each drug, using the CompuSyn software by Chou and Martin[43] based on the median-effect principle and plot.[44,45] The range of values given for vinblastine, taxol, and cisplatin are the mean ± SE (n = 4).

The in vitro cytotoxicity of sulfonates against human cancer cell lines HeLa-S3 (epithelial carcinoma), H460 (large-cell lung carcinoma), HT29 (colon adenocarcinoma), and PC-3 (prostate adenocarcinoma) were determined by assaying viable cell numbers using methylthiazole tetrazolium (WST-8) (Cell Count Kit 8, Dojindo Molecular Technologies Inc., Gaithersburg, MD, USA) as previously described.[46] Cells were seeded in a 96-well plate (3000 cells per well) and, 24 h later, were treated with sulfonate derivatives for 72 h. At the end of treatment, WST-8 was added to the medium and the plates were incubated at 37 °C for 1 h. Cell growth was determined by measuring the optical absorption of reduced formazan at 450 nm and expressing the result as a percentage of the absorption of the untreated control. The IC_{50} for each drug was determined from dose–effect relationships with six concentrations using GraphPad PRISM ver. 5.0 (GraphPad Inc., San Diego, CA, USA).

Analysis of cell cycle distribution

Cell cycle progression was monitored using DNA flow cytometry. DNA was stained with propidium iodide (PI), and mitotic cells were quantified by measuring the expression of the mitosis-specific marker phospho-histone H3, as previously described.[47] Phospho-histone H3 levels and the DNA content of individual cells were analyzed using a fluorescence-activated cell sorter (EpicsXL/MCL,

Beckman Coulter, Fullerton, CA), and the cell cycle distribution of the cells was determined using EXPO32 ADC Analysis software provided by Beckman Coulter.

Detection of apoptosis

Apoptotic cells were identified by flow cytometry analysis of the level of cleaved poly(ADP-ribose) polymerase (PARP).[48] Briefly, cells were fixed with ice-cold 70% EtOH for 16 h, then immunostained for 3 h at room temperature with rabbit anti-human cleaved PARP antibodies (Cell Signaling Technology, Beverly, MA), followed by incubation for 1 h at room temperature with allophycocyanin-conjugated goat anti-rabbit IgG (Invitrogen). Cellular DNA was counterstained with PI. Levels of cleaved PARP and PI in individual cells were analyzed using a fluorescence-activated cell sorter, and the percentage of cells with cleaved PARP was determined using EXPO32 ADC Analysis software provided by Beckman Coulter.

Immunofluorescence staining

Cells seeded on glass cover slips were incubated for 14 h at 37 °C with or without drugs, washed twice with phosphate-buffered saline (PBS), and fixed in situ with 90% MeOH at −20 °C for 10 min. The cells were then immunostained for mitotic spindles with an anti-human α-tubulin antibody (Sigma, St. Louis, MO, USA) and for centrosomes with an anti-human γ-tubulin antibody (Sigma) as previously described.[47] Nuclei were simultaneously counterstained with 0.1 μg mL^{-1} of 4,6-diamino-2-phenylindole (DAPI, Sigma). After thorough rinsing with PBS containing 0.2% (*v/v*) Tween 20, the cells were mounted using a 90% glycerol solution and examined under a fluorescence microscope (Axioskop 2, Zeiss, Oberkochen, Germany).

Cellular microtubule stabilization assay

The effect of sulfonate derivatives on microtubule stabilization was assessed using the cellular microtubule stabilization assay.[49] After treatment with the indicated compounds, HeLa-S3 cells were harvested in lysis buffer (100 mM PIPES pH 6.9, 1 mM EGTA, 1 mM $MgCl_2$, 30% glycerol, 0.5% DMSO, 1% NP-40, 1 mM GTP, and protease inhibitors). Following centrifugation at 180 000 *g* at 37 °C for 1 h, the polymerized tubulin fraction (pellet) and the soluble tubulin fraction (supernatant) were separated. These two fractions were adjusted to the same volume with Laemmli sample buffer. Finally, the amount of α-tubulin from equal aliquots of the polymerized tubulin fraction and the soluble tubulin fraction was determined by immunoblot analyses. Mitotic cells, released for 10 h from a double-thymidine block, were used as a control.

Determination of intrinsic tryptophan fluorescence of tubulin

Intrinsic tryptophan fluorescence of tubulin was used to measure the binding affinity of drugs to tubulin.[50] Porcine brain tubulin (3 μM, Cytoskeleton Inc., Denver, CO, USA) was incubated with the indicated drugs at 37 °C for 40 min in buffer containing 80 mM PIPES pH 6.9, 0.5 mM EGTA, and 2 mM $MgCl_2$. The samples were then excited at 295 nm, and the emission spectrum was monitored from 325 nm to 370 nm with a spectrofluorimeter (SpectraMax M5, Molecular Devices, Sunnyvale, CA, USA).

Colchicine competitive binding assay

The ability of the compounds to compete with colchicine for binding to tubulin was assessed by measuring the change in fluorescence of the tubulin–colchicine complex.[34] Tubulin (5 μM) was pre-incubated with 20 μM quinoline sulfonates, 20 μM colcemid (Sigma), or 20 μM vinblastine (Sigma) for 45 min at 37 °C. Next, 20 μM colchicine (Sigma) was added to all reaction mixtures. Spectra were recorded after 20 min incubation by exciting the samples at 360 nm and measuring emission at 435 nm using a spectrofluorimeter (SpectraMax M5, Molecular Devices).

BODIPY FL-vinblastine competitive binding assay

The ability of the compounds to compete with vinblastine for binding to tubulin was assessed by measuring the change in fluorescence of the BODIPY FL-vinblastine–tubulin complex. Tubulin (3 μM) was pre-incubated with either 20 μM quinoline sulfonate or 20 μM vinblastine for 45 min in buffer containing 80 mM PIPES pH 6.9, 0.5 mM EGTA and 2 mM $MgCl_2$, followed by the addition of BODIPY FL-vinblastine (3 μM, Invitrogen, Carlsbad, CA). After 20 min incubation, the samples were excited at 490 nm and emission spectra were monitored from 505 nm to 530 nm using a spectrofluorimeter (SpectraMax M5, Molecular Devices).

Abbreviations

CA-4, combretastatin A-4; CCRF-CEM, human lymphoblastic leukemia; DAPI, 4,6-diamino-2-phenylindole; DMF, *N*,*N*-dimethylformamide; HCT-116, human colon carcinoma; HeLa-S3, human epithelial carcinoma; H460, human large-cell lung carcinoma; HT29, human colon adenocarcinoma; MDR, multidrug resistance; PARP, poly(ADP-ribose) polymerase; PBS, phosphate-buffered saline; PC-3, prostate adenocarcinoma; PI, propidium iodide; SAR, structure–activity relationship.

Acknowledgements

We are grateful for support from the National Science Council, Taiwan, Republic of China (NSC 98-2320-B-001-005 to T.-L.S. and NSC 99-2320-B-001-008-MY3 to L.-H.Y.). T.-C.C. was supported by the Sloan-Kettering Institute General Fund. NMR spectra of synthesized compounds were obtained at the High-Field Biomolecular NMR Core Facility supported by the National Research Program for Genomic Medicine (Taiwan). We thank Dr. Shu-Chuan Jao at the Institute of Biological Chemistry (Academia Sinica) for providing NMR service and the National Center for High-Performance Computing for computer time and facilities.

Keywords: antitumor agents · cytotoxicity · mitotic arrest · sulfonates · tubulin polymerization

[1] K. H. Downing, E. Nogales, *Curr. Opin. Cell Biol.* **1998**, *10*, 16–22.
[2] M. A. Jordan, L. Wilson, *Nat. Rev. Cancer* **2004**, *4*, 253–265.
[3] J. R. McIntosh, E. L. Grishchuk, R. R. West, *Annu. Rev. Cell Dev. Biol.* **2002**, *18*, 193–219.
[4] S. Honore, E. Pasquier, D. Braguer, *Cell Mol. Life Sci.* **2005**, *62*, 3039–3056.
[5] F. Pellegrini, D. R. Budman, *Cancer Invest.* **2005**, *23*, 264–273.

[6] M. A. Jordan, *Curr. Med. Chem. Anticancer Agents* **2002**, *2*, 1 – 17.
[7] K. E. Gascoigne, S. S. Taylor, *J. Cell Sci.* **2009**, *122*, 2579 – 2585.
[8] O. Pauwels, R. Kiss, J. L. Pasteels, G. Atassi, *J. Pharm. Pharmacol.* **1995**, *47*, 870 – 875.
[9] I. Ringel, S. B. Horwitz, *J. Natl. Cancer Inst.* **1991**, *83*, 288 – 291.
[10] T.-C. Chou, H. Dong, X. Zhang, W. P. Tong, S. J. Danishefsky, *Cancer Res.* **2005**, *65*, 9445 – 9454.
[11] E. Hamel, *Med. Res. Rev.* **1996**, *16*, 207 – 231.
[12] K. H. Downing, *Annu. Rev. Cell Dev. Biol.* **2000**, *16*, 89 – 111.
[13] C. Dumontet, B. I. Sikic, *J. Clin. Oncol.* **1999**, *17*, 1061 – 1070.
[14] G. R. Pettit, G. M. Cragg, D. L. Herald, J. M. Schmidt, P. Lohavanijaya, *Can. J. Chem.* **1982**, *60*, 1374 – 1376.
[15] G. R. Pettit, S. B. Singh, E. Hamel, C. M. Lin, D. S. Alberts, D. Garcia-Kendall, *Experientia* **1989**, *45*, 209 – 211.
[16] A. A. el-Zayat, D. Degen, S. Drabek, G. M. Clark, G. R. Pettit, D. D. Von Hoff, *Anticancer Drugs* **1993**, *4*, 19 – 25.
[17] A. Chaudhary, S. N. Pandeya, P. Kumar, P. P. Sharma, S. Gupta, N. Soni, K. K. Verma, G. Bhardwaj, *Mini-Rev. Med. Chem.* **2007**, *7*, 1186 – 1205.
[18] C. M. Lin, H. H. Ho, G. R. Pettit, E. Hamel, *Biochemistry* **1989**, *28*, 6984 – 6991.
[19] G. R. Pettit, S. B. Singh, M. R. Boyd, E. Hamel, R. K. Pettit, J. M. Schmidt, F. Hogan, *J. Med. Chem.* **1995**, *38*, 1666 – 1672.
[20] R. T. Dorr, K. Dvorakova, K. Snead, D. S. Alberts, S. E. Salmon, G. R. Pettit, *Invest. New Drugs* **1996**, *14*, 131 – 137.
[21] G. R. Pettit, D. Temple, Jr., V. L. Narayanan, R. Varma, M. J. Simpson, M. R. Boyd, G. A. Rener, N. Bansal, *Anticancer Drug Des.* **1995**, *10*, 299 – 309.
[22] G. R. Pettit, M. R. Rhodes, *Anticancer Drug Des.* **1998**, *13*, 183 – 191.
[23] A. Dowlati, K. Robertson, M. Cooney, W. P. Petros, M. Stratford, J. Jesberger, N. Rafie, B. Overmoyer, V. Makkar, B. Stambler, A. Taylor, J. Waas, J. S. Lewin, K. R. McCrae, S. C. Remick, *Cancer Res.* **2002**, *62*, 3408 – 3416.
[24] J. W. Lippert III, *Bioorg. Med. Chem.* **2007**, *15*, 605 – 615.
[25] G. C. Tron, T. Pirali, G. Sorba, F. Pagliai, S. Busacca, A. A. Genazzani, *J. Med. Chem.* **2006**, *49*, 3033 – 3044.
[26] S. L. Gwaltney II, H. M. Imade, K. J. Barr, Q. Li, L. Gehrke, R. B. Credo, R. B. Warner, J. Y. Lee, P. Kovar, J. Wang, M. A. Nukkala, N. A. Zielinski, D. Frost, S. C. Ng, H. L. Sham, *Bioorg. Med. Chem. Lett.* **2001**, *11*, 871 – 874.
[27] A. Zuse, P. Schmidt, S. Baasner, K. J. Bohm, K. Muller, M. Gerlach, E. G. Gunther, E. Unger, H. Prinz, *J. Med. Chem.* **2007**, *50*, 6059 – 6066.
[28] S. C. Kuo, H. Z. Lee, J. P. Juang, Y. T. Lin, T. S. Wu, J. J. Chang, D. Lednicer, K. D. Paull, C. M. Lin, E. Hamel, K. H. Lee, *J. Med. Chem.* **1993**, *36*, 1146 – 1156.
[29] L. Li, H. K. Wang, S. C. Kuo, T. S. Wu, D. Lednicer, C. M. Lin, E. Hamel, K. H. Lee, *J. Med. Chem.* **1994**, *37*, 1126 – 1135.
[30] L. Li, H. K. Wang, S. C. Kuo, T. S. Wu, A. Mauger, C. M. Lin, E. Hamel, K. H. Lee, *J. Med. Chem.* **1994**, *37*, 3400 – 3407.
[31] K. Chen, S. C. Kuo, M. C. Hsieh, A. Mauger, C. M. Lin, E. Hamel, K. H. Lee, *J. Med. Chem.* **1997**, *40*, 2266 – 2275.
[32] K. Chen, S. C. Kuo, M. C. Hsieh, A. Mauger, C. M. Lin, E. Hamel, K. H. Lee, *J. Med. Chem.* **1997**, *40*, 3049 – 3056.
[33] G. Pifferi, R. Monguzzi, *J. Pharm. Sci.* **1973**, *62*, 1392.
[34] B. Bhattacharyya, J. Wolff, *Proc. Natl. Acad. Sci. USA* **1974**, *71*, 2627 – 2631.
[35] P. S. Sardar, S. S. Maity, L. Das, S. Ghosh, *Biochemistry* **2007**, *46*, 14544 – 14556.
[36] S. Mukherjee, B. R. Acharya, B. Bhattacharyya, G. Chakrabarti, *Biochemistry* **2010**, *49*, 1702 – 1712.
[37] L. Seed, D. P. Slaughter, L. R. Limarzi, *Surgery* **1940**, *7*, 696 – 709.
[38] J. A. Hadfield, S. Ducki, N. Hirst, A. T. McGown, *Prog. Cell. Cycle Res.* **2003**, *5*, 309 – 325.
[39] J. Zhou, P. Giannakakou, *Curr. Med. Chem. Anticancer Agents* **2005**, *5*, 65 – 71.
[40] D. A. Scudiero, R. H. Shoemaker, K. D. Paull, A. Monks, S. Tierney, T. H. Nofziger, M. J. Currens, D. Seniff, M. R. Boyd, *Cancer Res.* **1988**, *48*, 4827 – 4833.
[41] P. Skehan, R. Storeng, D. Scudiero, A. Monks, J. McMahon, D. Vistica, J. T. Warren, H. Bokesch, S. Kenney, M. R. Boyd, *J. Natl. Cancer Inst.* **1990**, *82*, 1107 – 1112.
[42] T.-C. Chou, O. A. O'Connor, W. P. Tong, Y. Guan, Z. G. Zhang, S. J. Stachel, C. Lee, S. J. Danishefsky, *Proc. Natl. Acad. Sci. USA* **2001**, *98*, 8113 – 8118.
[43] T.-C. Chou, N. Martin, *CompuSyn Software*, CompuSyn Inc., Paramus, NJ (USA), **2005**.
[44] T.-C. Chou, P. Talalay, *Adv. Enzyme Regul.* **1984**, *22*, 27 – 55.
[45] T.-C. Chou, *Pharmacol. Rev.* **2006**, *58*, 621 – 681.
[46] R. Hori, M. Kashiba, T. Toma, A. Yachie, N. Goda, N. Makino, A. Soejima, T. Nagasawa, K. Nakabayashi, M. Suematsu, *J. Biol. Chem.* **2002**, *277*, 10712 – 10718.
[47] L. H. Yih, Y. Y. Tseng, Y. C. Wu, T. C. Lee, *Cancer Res.* **2006**, *66*, 2098 – 2106.
[48] X. Li, Z. Darzynkiewicz, *Exp. Cell Res.* **2000**, *255*, 125 – 132.
[49] S. H. Zhuang, Y. E. Hung, L. Hung, R. W. Robey, D. L. Sackett, W. M. Linehan, S. E. Bates, T. Fojo, M. S. Poruchynsky, *Clin. Cancer Res.* **2007**, *13*, 7480 – 7486.
[50] A. R. Prasad, R. F. Luduena, P. M. Horowitz, *Biochemistry* **1986**, *25*, 3536 – 3540.

Received: March 1, 2011
Revised: April 1, 2011
Published online on May 3, 2011

